



LJMU Research Online

Lee, JSH, Wich, SA, Widayati, A and Koh, LP

Detecting industrial oil palm plantations on Landsat images with Google Earth Engine

<http://researchonline.ljmu.ac.uk/id/eprint/4807/>

Article

Citation (please note it is advisable to refer to the publisher's version if you intend to cite from this work)

Lee, JSH, Wich, SA, Widayati, A and Koh, LP (2016) Detecting industrial oil palm plantations on Landsat images with Google Earth Engine. Remote Sensing Applications: Society and Environment. ISSN 2352-9385

LJMU has developed **LJMU Research Online** for users to access the research output of the University more effectively. Copyright © and Moral Rights for the papers on this site are retained by the individual authors and/or other copyright owners. Users may download and/or print one copy of any article(s) in LJMU Research Online to facilitate their private study or for non-commercial research. You may not engage in further distribution of the material or use it for any profit-making activities or any commercial gain.

The version presented here may differ from the published version or from the version of the record. Please see the repository URL above for details on accessing the published version and note that access may require a subscription.

For more information please contact researchonline@ljmu.ac.uk

<http://researchonline.ljmu.ac.uk/>

1 **Detecting industrial oil palm plantations on Landsat images with Google Earth Engine**

2 Janice Ser Huay Lee¹, Serge Wich^{2,3}, Atiek Widayati⁴, Lian Pin Koh⁵

3 ¹ *Asian School of the Environment, Nanyang Technological University of Singapore,*
4 *Singapore*

5 ² *School of Natural Sciences and Psychology, Liverpool John Moores University, United*
6 *Kingdom*

7 ³ *Institute for Biodiversity and Ecosystem Dynamics, University of Amsterdam, The*
8 *Netherlands*

9 ⁴ *World Agroforestry Centre, Jl CIFOR, Situ Gede, Sindang Barang, Bogor, Indonesia*

10 ⁵ *Environment Institute, and School of Earth and Environmental Sciences, University of*
11 *Adelaide, Australia*

12

13 **Short running title:** Oil palm detection using Google Earth Engine

14 **Word count:** 3327 words (excluding abstract and references)

15 **Authors' names and addresses:**

16 Janice Ser Huay Lee, *Asian School of the Environment, Nanyang Technological University of*
17 *Singapore, Singapore.* janice.jlsh@gmail.com

18 Serge Wich, *School of Natural Sciences and Psychology, Liverpool John Moores University,*
19 *United Kingdom,* s.a.wich@ljmu.ac.uk

20 Atiek Widayati, *World Agroforestry Centre, Jl CIFOR, Situ Gede, Sindang Barang, Bogor,*
21 *Indonesia,* A.Widayati@cgiar.org

22 Lian Pin Koh, *Environment Institute, and School of Earth and Environmental Sciences,*
23 *University of Adelaide,* lianpin.koh@adelaide.edu.au

24

25 **Full contact details of corresponding author:**

26 Janice Ser Huay Lee

27 Address: Asian School of the Environment, Nanyang Technological University of Singapore,

28 50 Nanyang Avenue, Block N2-01C-43, Singapore 639798

29 Email: janice.jlsh@gmail.com

30 **Abstract:**

31 Oil palm plantations are rapidly expanding in the tropics, which leads to deforestation and
32 other associated damages to biodiversity and ecosystem services. Forest researchers and
33 practitioners in developing nations are in need of a low-cost, accessible and user-friendly tool
34 for detecting the establishment of industrial oil palm plantations. Google Earth Engine (GEE)
35 is a cloud computing platform which hosts publicly available satellite images and allows for
36 land cover classification using inbuilt algorithms. These algorithms conduct pixel-based
37 classification via supervised learning. We demonstrate the use of GEE for the detection of
38 industrial oil palm plantations in Tripa, Aceh, Indonesia. We performed land cover
39 classification using different spectral bands (RGB, NIR, SWIR, TIR, all bands) from our
40 Landsat 8 image to distinguish the following land cover classes: immature oil palm, mature
41 oil palm, non-forest non-oil palm, forest, water, and clouds. The overall accuracy and Kappa
42 coefficient were the highest using all bands for land cover classification, followed by RGB,
43 SWIR, TIR, and NIR. Classification and Regression Trees (CART) and Random Forests
44 (RFT) algorithms produced classified land cover maps which had higher overall accuracies
45 and Kappa coefficients than the Minimum Distance (MD) algorithm. Object-based
46 classification and using a combination of radar- and optic-based imagery are some ways in
47 which oil palm detection can be improved within GEE. Despite its limitations, GEE does
48 have the potential to be developed further into an accessible and low-cost tool for
49 independent bodies to detect and monitor the expansion of oil palm plantations in the tropics.

50 **Key-words:** *Elaeis guineensis*, agricultural expansion, tropics, land cover classification, land
51 use change

52 **Detecting industrial oil palm plantations on Landsat images with Google Earth Engine**

53 **1. Introduction**

54 The oil palm (*Elaeis guineensis*) has become one of the most rapidly expanding equatorial
55 crops in the world, with the global extent of oil palm cultivation increasing from 3.6 million
56 ha in 1961 to 17.2 million ha in 2012 (FAOSTAT, 2014). Due to its multiple uses for food
57 and industrial products, global demand for palm oil has increased over the last few decades,
58 and has spurred both private and government sectors to invest heavily in the oil palm industry
59 (World Bank, 2011). While oil palm production has an important role in rural development
60 and supporting local and regional economies (World Bank, 2010), the rapid expansion of
61 industrial oil palm plantations has also led to detrimental social and environmental impacts,
62 especially in the region of Southeast Asia (Sheil et al., 2009), but such impacts are a growing
63 concern in Africa as well (Wich et al., 2014).

64 Over the last few decades, tropical deforestation as a result of oil palm expansion has
65 been rapid and extensive (Carlson et al., 2013; Koh et al., 2011; Uryu et al., 2008). In
66 Kalimantan, the Indonesian side of Borneo, it is estimated that oil palm plantations were
67 directly responsible for ~57% of 2000 - 2010 deforestation (Carlson et al., 2013); while in
68 Sumatra, deforestation within oil palm concessions accounted for ~19% of 2000 - 2010
69 deforestation (Lee et al., 2013). Industrial oil palm plantations have also been singled out for
70 impacting peat ecosystems which are important carbon sinks in Peninsular Malaysia, Borneo,
71 and Sumatra (Koh, Miettinen, Liew, & Ghazoul, 2011; Miettinen et al., 2012). Conversion of
72 tropical forests to oil palm plantations leads to biodiversity losses (Fitzherbert et al., 2008),
73 higher carbon dioxide emissions (Dewi et al., 2009), and warmer stream environments as
74 well as higher sedimentation in aquatic systems (Carlson et al., 2014). As forests around the
75 world are increasingly exploited and subsequently converted for oil palm plantations (Butler,

76 2013; Hoyle and Levang, 2012), it is important to have a classification system which is able
77 to detect oil palm land cover across the tropics in near real-time.

78 Mapping of oil palm land cover using satellite remote sensing data has been carried
79 out in many studies across the tropics (Gutiérrez-Vélez et al., 2011; Li et al., 2015; Miettinen
80 and Liew, 2010; Shafri et al., 2011; Srestasathiern and Rakwatin, 2014). There are two broad
81 categories of using optics based methods to study land cover classification from remote
82 sensing data: phenology-based and image-based methods (Li et al., 2015). Phenology-based
83 methods such as Gutiérrez-Vélez et al. (2011) use temporal changes in vegetation greenness
84 to detect the area deforested by large-scale oil palm expansion in the Peruvian Amazon.
85 Image-based methods utilize spectral signatures as well as textural information to
86 differentiate oil palm trees from their surroundings (Carlson et al., 2013; Thenkabail et al.,
87 2004). Oil palm plantations can be manually digitized from satellite images, based on the
88 unique textural information of oil palm plantations (e.g., long rectangular blocks for
89 industrial plantations, geometric shape of oil palm canopy, presence of roads) along with
90 expert knowledge on the land use system (Carlson et al., 2013; Uryu et al., 2008). Other
91 studies have also tried to automate the detection of oil palm plantations based on spectral
92 image analysis which classifies pixels based on their spectral class thresholds (Shafri et al.,
93 2011). Some challenges related to detecting oil palm plantations using optics based methods
94 include the difficulty in separating oil palm plantations from other spectrally similar land
95 cover types (e.g., forests, rubber trees) (Morel et al., 2011) as well as the frequent presence of
96 cloud cover in the tropics which hinders image analysis (Li et al., 2015). Recent use of radar
97 data which is all-weather and all-time capable has shown great potential and suitability for oil
98 palm mapping (Miettinen and Liew, 2010). Phased Array type L-band Synthetic Aperture
99 Radar (PALSAR) data has been used by Miettinen and Liew (2010) for distinguishing
100 between woody plantations including rubber (*Hevea brasiliensis*), wattles (*Acacia spp.*), and

101 palms (oil palm and coconut (*Cocos nucifera*)). The use of both radar and optical data for
102 image classification may provide enhanced information on land cover and use (Joshi et al.,
103 2016). Microwave energy scattered by vegetation depends on the size, density, as well as
104 orientation and dielectric properties of elements that are comparable to the size of the radar
105 wavelength, while optical energy reflected by vegetation depends on the leaf structure,
106 pigmentation and moisture (Joshi et al., 2016). Hence, radar data provide more information
107 on the structural properties of the land, while optical products, commonly available in the
108 form of multispectral images, offer information on spectral reflectance and can be used to
109 accentuate land cover using different indices (e.g., Normalized Difference Vegetation Index)
110 (Joshi et al., 2016).

111 These methods of classifying oil palm land cover require training in remote sensing,
112 expensive software to process satellite images, and expensive hardware with fast computer
113 processing power and large storage capacities (Friess et al., 2011). While it is important that
114 such mapping exercises be carried out cautiously, these methods do require a significant
115 amount of time, and are disadvantageous for independent monitoring bodies (e.g.,
116 environmental non-governmental organizations (NGOs) in developing countries) which wish
117 to monitor oil palm expansion in tropical landscapes. An increasing number of producer and
118 consumer companies have pledged to purchase certified sustainable palm oil to ensure that
119 their supply chains do not involve tropical deforestation or zero-deforestation policies (May-
120 Tobin et al., 2012). Certified sustainable palm oil is produced based on a set of environmental
121 and social criteria set out by a standards body such as the Roundtable of Sustainable Palm Oil
122 (RSPO; <http://www.rspo.org/>). The use of earth observation technologies is one of the ways
123 to monitor the credibility of producer companies who have pledged themselves to zero-
124 deforestation policies.

125 The advent of digital globes such as Google Earth has played an important role in
126 facilitating public access to geospatial analysis and simple spatial analysis tools (Butler,
127 2006; Friess et al., 2011). Google Earth Engine (GEE) (<http://earthengine.google.org>) takes
128 open source geospatial analysis one step further by providing a cloud computing platform for
129 earth observation data analysis. It combines a public data catalogue, which consists of a
130 nearly complete set of Landsat imagery from its start in 1972 until the present day, with a
131 large-scale computational facility optimized for parallel processing of geospatial data
132 (Hansen et al., 2013). In a recent global forest mapping exercise by Hansen et al. (2013), a
133 total of 20 terapixels of Landsat data were processed on GEE, using one million CPU-core
134 hours on 10,000 computers in parallel, in order to characterize year 2000 percent tree cover
135 and subsequent tree cover loss and gain through 2012. This process was completed in a
136 matter of days on GEE but would have taken 15 years for a single computer to finish
137 (<http://googleresearch.blogspot.ch/2013/11/the-first-detailed-maps-of-global.html>). GEE also
138 hosts an imagery classification system in the cloud which enables one to run supervised
139 learning algorithms across huge datasets in real time. These algorithms are trained to identify
140 different land cover classes using hand-drawn points and polygons on the input dataset
141 (satellite image). This land cover classification method is rapid and accessible through the
142 World Wide Web. Hence, GEE's computing infrastructure revolutionizes time-consuming
143 remote sensing processes, facilitates access of remote sensing resources and tools to the
144 public, and paves a new way forward for rapid land cover classification.

145 To explore the potential of GEE's imagery classification system as a low-cost,
146 accessible and user-friendly oil palm detection tool, we used GEE's classifiers to detect and
147 map the establishment of industrial oil palm plantations in Aceh province, Indonesia. To
148 assess the performance of GEE's classification methods, we verified land cover maps
149 produced by GEE with a set of randomly selected training points. In so doing, we aim to

150 evaluate GEE as a potential oil palm monitoring system for scientists and NGOs in tropical
151 developing countries.

152

153 **2. Study site**

154 Our study site is located at Tripa (3°50'31 N, 96°33'17 E), which is on the west coast of
155 Aceh province, Indonesia. The Tripa landscape covers an area of ~1,020 km², and falls under
156 the administration of two districts, Nagan Raya and Aceh Barat Daya. Our study area (314
157 km²) is part of the Tripa landscape. In the early 1990s, Tripa was covered with pristine peat
158 swamp forests and hosted as many as 1,000 Sumatran orangutans (*Pongo abelii*) (Wich et al.,
159 2011). This landscape is characterized by large peat domes and deep peat with peat depth
160 greater than 3 meters (Wich et al., 2011). However over the last two and a half decades, the
161 Tripa ecosystem has seen a rapid decline in forest cover mainly due to oil palm agricultural
162 expansion at both the scale of industrial and smallholder plantations (Tata et al., 2010). Due
163 to the predominance of oil palm agriculture in this landscape and rapid transitions of forest to
164 oil palm land cover, we used Tripa as a case study for testing GEE's imagery classification
165 system for detecting industrial oil palm plantations.

166

167 **3. Data and Methods**

168 We searched for Landsat 8 top-of-atmosphere reflectance (TOA) images from 1st January
169 2014 to 31st December 2014 from GEE's data catalogue and selected the image with the least
170 cloud cover as the image used for supervised classification of oil palm land cover. Landsat 8
171 images are taken every 16 days and have a resolution of 30 m, making them useful for
172 monitoring land cover change over time.

173 We aimed to assess GEE's ability to separate immature oil palm, mature oil palm,
174 non-forest non-oil palm, and forest land cover classes. We plotted 450 training points for

175 each land cover class. The classes of the training points were specified by the lead author
176 who has experience working in Tripa and is familiar with the land cover in this landscape.
177 We first identified industrial oil palm plantations using rectangular grid lines which indicate
178 oil palm development (Uryu et al., 2008). Of these plantations, ‘Immature Oil Palm’
179 displayed a lighter shade of green compared to ‘Mature Oil Palm’. In the absence of
180 rectangular grid lines which indicate the absence of industrial oil palm development, burnt
181 areas and vegetation mosaics were classified under ‘Non-forest non-oil palm’ land cover.
182 ‘Forest’ land cover displayed a contiguous vegetation cover with a dark shade of green. Other
183 additional land cover classes included ‘Water’ and ‘Clouds’.

184 We used 60% of these training points to train the GEE classifiers while the remaining
185 40% were used to conduct accuracy assessments. We used different spectral bands from the
186 Landsat 8 TOA image for image classification. We included red, green and blue bands
187 (RGB), Near Infra-Red (NIR), Short Wave Infra-Red (SWIR), Thermal Infra-Red (TIR), and
188 all bands (including RGB, NIR, SWIR and TIR) for image classification. During image
189 classification, all pixels in the input image were assigned to a class, according to their
190 spectral signature. GEE has 10 classifiers, CART, Random Forest, Minimum Distance, GMO
191 MaxEnt, Naïve Bayes, SVM, Perceptron, IKPamir, and Winnow, for image classification.
192 Each of these classifiers uses a different algorithm to assign pixels to classes and perform
193 land cover classification in a pixel-based manner. Out of the nine classifiers listed above,
194 GMO MaxEnt, Naïve Bayes, SVM, Perceptron, IKPamir and Winnow produced land cover
195 maps which had little distinction among the different classes. Hence, we excluded the above
196 six classifiers and compared GEE maps produced by classifiers CART, Random Forest, and
197 Minimum Distance (Table 1).

198 A validation error matrix was produced in GEE and the overall, producer’s and user’s
199 accuracy were calculated. Since we were more interested in understanding how GEE

200 classification detects industrial oil palm, we focused more on the producer's and user's
201 accuracy for immature and mature oil palm land cover classes. We calculated the Kappa
202 coefficient which tests whether a land cover map is significantly better than if a map had been
203 generated at random (Congalton, 1996). Kappa values are generally characterized into 3
204 groupings: 0.80 represents strong agreement, 0.40-0.80 represents moderate agreement, and
205 below 0.40 represents poor agreement (Congalton, 1996). However, the Kappa coefficient
206 has come under recent question as a useful metric for accuracy assessments (Pontius and
207 Millones, 2011), and should be interpreted with caution. All geospatial analyses were
208 conducted in GEE API (<https://code.earthengine.google.com/>). The Earth Engine code for
209 this analysis is available under Supplementary Material.

210

211 **4. Results**

212 GEE classifiers are able to detect industrial oil palm land cover from Landsat 8 images. In
213 particular, the CART and Random Forest (RFT) classifiers provided the highest overall
214 accuracy scores using ALL bands and RGB bands and outperformed the Minimum Distance
215 (MD) classifier (Table 2; Figure 1). Based on the overall accuracy scores, CART
216 classification using ALL bands came in first (93.6% with a Kappa coefficient of 0.92),
217 followed by Random Forest (RFT) classification using ALL bands (91.2% with a Kappa
218 coefficient of 0.89), and CART classification using RGB bands (Table 2). The near infrared
219 (NIR) and thermal infrared (TIR) bands performed poorly compared to the ALL, RGB and
220 SWIR bands.

221 GEE classifiers CART and RFT using ALL and RGB bands provided the best producer's and
222 user's accuracy scores for distinguishing immature oil palm (Table 3). The producer's
223 accuracy for immature oil palm was the highest under the CART classifier using ALL bands
224 (94%), followed by the RFT classifier using ALL bands (88%), and RFT classifier using

225 RGB bands (83%). The user's accuracy for immature oil palm was highest for CART
226 classifier using RGB bands (92%), followed by CART classifier using ALL bands (88%),
227 and RFT classifier using RGB bands (86%).
228 GEE classifiers CART and RFT using ALL and RGB bands also provided the best producer's
229 and user's accuracy scores for distinguishing mature oil palm (Table 3). Interestingly, the
230 producer's accuracy score for MD classifier using SWIR bands was the second highest
231 (Table 3). The producer's accuracy for mature oil palm was highest for CART classifier
232 using ALL bands, followed by MD classifier using SWIR bands (82%), and RFT classifier
233 using ALL bands (80%). The user's accuracy for mature oil palm was highest for CART
234 classifier using ALL bands (88%), followed by RFT classifier using ALL bands (87%), and
235 RFT classifier using RGB bands (71%).

236

237 **5. Discussion**

238 GEE classifiers are able to detect industrial oil palm land cover from Landsat 8 images,
239 which are a useful source of publicly available satellite images for near real-time monitoring
240 of land use change. Based on the high overall accuracy and moderate Kappa coefficients,
241 CART and RFT classifiers outperformed the MD classifier to produce classified land cover
242 images of an oil palm dominated landscape. Under MD classification, the spectral distance
243 between the measurement vector for the candidate pixel and the mean vector for each
244 signature is calculated, and the class of the candidate pixel is then assigned to the class for
245 which the spectral distance is the lowest. Hence, the MD approach works well when the
246 distance between the means is large compared to the spread of each class with respect to its
247 mean. Since the land cover classes being segregated here are very similar (immature oil palm,
248 mature oil palm, non-forest non-oil palm, forest), the distance between the means may be
249 small and result in the poor performance of the MD classifier. In contrast, CART and RFT

250 classifiers are machine learning classifiers and use a decision tree as a predictive model to
251 classify candidate pixels into classes. They are strictly nonparametric and are less sensitive to
252 the distributions of the input data (Friedl and Brodley, 1997).

253 While near infrared bands from high resolution imagery have been used to
254 successfully detect diseases in oil palm trees (Santoso et al., 2011; Shafri et al., 2011;
255 Thenkabail et al., 2004), they are less useful in itself for distinguishing land cover classes in
256 our study. The use of both infrared bands and visual bands (ALL) as well as visual bands
257 themselves were most useful in distinguishing land cover classes in our study. Distinguishing
258 oil palm plantations from secondary vegetation and flooded forests has been shown to be a
259 challenge due to both land covers being spectrally and structurally similar (Morel et al., 2011;
260 Santos and Messina, 2008). Hence pixel-based image analysis without the use of non-spectral
261 information such as the shape and texture of the image pixels may be insufficient for
262 detecting oil palm plantations. In the case of differentiating industrial oil palm from forests,
263 an object-based classification approach, which takes into consideration spectral, shape and
264 contextual relationships of groups of image pixels, will be more effective (Carlson et al.,
265 2013; Uryu et al., 2008). A combination of PALSAR and Landsat images have also been
266 shown to be effective for differentiating oil palm plantations from forests (Li et al., 2015;
267 Miettinen and Liew, 2010). Synthetic Aperture Radar (SAR) data from the European Union
268 Space Agency is available on GEE and can be considered in combination with Landsat
269 images for future detection of industrial oil palm plantations. Detecting immature oil palm
270 and smallholder oil palm plantations is an important area for future research to detect oil
271 palm expansion in its early phase, and for keeping track of smallholder-led expansion which
272 is occurring more frequently in places such as Cameroon (Nkongho et al., 2014) and
273 Sumatra, Indonesia (Ekadinata et al., 2013).

274 Our results show the potential use of GEE's imagery classification system as a tool
275 for oil palm land cover mapping but also reveal the limitations of this classification system
276 especially in relation to the level of accuracy for detecting immature and mature oil palm
277 plantations from other land cover types with similar spectral signatures. In most oil palm
278 mapping studies, manual digitization of satellite imagery, accompanied by intensive field
279 visits are commonly employed to detect oil palm from other land cover types (Carlson et al.,
280 2013; Uryu et al., 2008). Such techniques ensure a higher level of accuracy and are able to
281 differentiate immature, young plantations from other land cover types such as shrub or
282 agricultural land. However, such high level accuracy mapping techniques also require
283 substantial expertise, resources and time, which is difficult to do on a frequent basis. Hence,
284 there is a tradeoff between time and resources, and the level of accuracy of oil palm mapping
285 within GEE's imagery classification system. The oil palm classification method demonstrated
286 in GEE is useful to provide a quick understanding of oil palm plantations present in the
287 landscape. This in itself is advantageous for independent monitoring bodies to conduct a
288 survey of the landscape in question and conduct more detailed assessments if necessary.

289 In this study, we assessed the use of GEE's classifiers for detecting industrial oil palm
290 plantations in Tripa, Indonesia. Expanding the scope of our study to include other regions of
291 Indonesia (e.g., Kalimantan and Papua) as well as other parts of the world (e.g., Cameroon
292 and Peru where oil palm is expanding rapidly (Butler, 2013; Mousseau, 2013)) would be a
293 useful next step to test GEE's oil palm mapping for different contexts of oil palm
294 development. The ultimate goal would be to develop an online tool where preliminary
295 detection of mature, industrial oil palm plantations can be made publicly available to various
296 stakeholders (e.g., researchers, non-governmental organizations, government officials, as well
297 as industry players) to increase monitoring efforts and improve transparency on whether palm
298 oil production is linked to tropical deforestation. Hence, a near real-time detection for oil

299 palm expansion will allow for better monitoring of oil palm expansion within the tropics, and
300 has potential implications for the traceability of zero-deforestation palm oil products. Despite
301 its limitations, GEE classification system does have the potential to be developed further into
302 an accessible and low-cost tool for detecting industrial oil palm plantations in the tropics.

303

304 **Acknowledgements**

305 We thank David Thau for providing us access to Google Earth Engine under the Trusted
306 Tester Program. We thank Christiaan Adams and staff from the Google Earth Engine
307 Development team for their input and assistance with the API code. We thank Burivalova Z.
308 for providing useful comments to the manuscript. L.P.K. is supported by the Australian
309 Research Council.

310

311 **References**

- 312 Butler, D., 2006. Virtual globes: The web-wide world. *Nature* 439, 776-778.
- 313 Online Database Butler, R., 2013. Palm oil company destroys 7,000 ha of Amazon rainforest in Peru,
314 Mongabay.com.
- 315 Carlson, K.M., Curran, L.M., Asner, G.P., Pittman, A.M., Trigg, S.N., Marion Adeney, J., 2013.
316 Carbon emissions from forest conversion by Kalimantan oil palm plantations. *Nature Climate*
317 *Change* 3, 283–287.
- 318 Carlson, K.M., Curran, L.M., Ponette-González, A., Ratnasari, D., Ruspita, P., Lisnawati, N.,
319 Purwanto, Y., Brauman, K.A., Raymond, P.A., 2014. Watershed-climate interactions influence
320 stream temperature, sediment yield, and metabolism along a land-use intensity gradient in
321 Indonesian Borneo. *Journal of Geophysical Research: Biogeosciences*, 2013JG002516.
- 322 Congalton, R.G., 1996. Accuracy assessment: a critical component of land cover mapping., In: Scott,
323 J.M., Tear, T.H., Davis, F. (Eds.), *Gap Analysis: A Landscape Approach to Biodiversity Planning*,
324 Bethesda, Maryland: American Society for Photogrammetry and Remote Sensing, pp. 119-131.
- 325 Dewi, S., Khasanah, N., Rahayu, S., Ekadinata, A., van Noordwijk, M., 2009. Carbon Footprint of
326 Indonesian Palm Oil Production: a Pilot Study.
- 327 Ekadinata, A., van Noordwijk, M., Budidarsono, S., Dewi, S., 2013. Hot spots in Riau, haze in
328 Singapore: the June 2013 event analyzed., ASB Partnership for the Tropical Forest Margins.
329 World Agroforestry Centre, Nairobi, Kenya.

330 Online DatabaseFAOSTAT, 2014. FAOSTAT Online Statistical Service. Food and Agriculture
331 Organization of the United Nations (FAO).

332 Fitzherbert, E.B., Struebig, M.J., Morel, A., Danielsen, F., Brühl, C.A., Donald, P.F., Phalan, B.,
333 2008. How will oil palm expansion affect biodiversity? *Trends Ecol Evol* 23, 538-545.

334 Friedl, M.A., Brodley, C.E., 1997. Decision tree classification of land cover from remotely sensed
335 data. *Remote Sensing of Environment* 61, 399-409.

336 Friess, D.A., Kudavidanage, E.P., Webb, E.L., 2011. The digital globe is our oyster. *Frontiers in*
337 *Ecology and the Environment* 9, 542-542.

338 Gutiérrez-Vélez, V.H., DeFries, R., Pinedo-Vásquez, M., Uriarte, M., Padoch, C., Baethgen, W.,
339 Fernandes, K., Lim, Y., 2011. High-yield oil palm expansion spares land at the expense of forests
340 in the Peruvian Amazon. *Environmental Research Letters* 6, 044029.

341 Hansen, M.C., Potapov, P.V., Moore, R., Hancher, M., Turubanova, S.A., Tyukavina, A., Thau, D.,
342 Stehman, S.V., Goetz, S.J., Loveland, T.R., Kommareddy, A., Egorov, A., Chini, L., Justice, C.O.,
343 Townshend, J.R.G., 2013. High-Resolution Global Maps of 21st-Century Forest Cover Change.
344 *Science* 342, 850-853.

345 Hoyle, D., Levang, P., 2012. Oil palm development in Cameroon, WWF (World Wildlife Fund for
346 Nature), IRD (Institut de Recherche pour le Développement, France), CIFOR (Centre for
347 International Forestry Research), WWF, Cameroon.

348 Joshi, N., Baumann, M., Ehammer, A., Fensholt, R., Grogan, K., Hostert, P., Jepsen, M., Kuemmerle,
349 T., Meyfroidt, P., Mitchard, E., Reiche, J., Ryan, C., Waske, B., 2016. A Review of the
350 Application of Optical and Radar Remote Sensing Data Fusion to Land Use Mapping and
351 Monitoring. *Remote Sensing* 8, 70.

352 Koh, L.P., Miettinen, J., Liew, S.C., Ghazoul, J., 2011. Remotely sensed evidence of tropical peatland
353 conversion to oil palm. *Proc. Natl Acad. Sci.* 108, 5127-5132.

354 Lee, J.S.H., Abood, S., Ghazoul, J., Barus, B., Obidzinski, K., Koh, L.P., 2013. Environmental
355 impacts of large-scale oil palm enterprises exceed that of smallholdings in Indonesia. *Conserv*
356 *Lett*, doi: 10.1111/conl.12039.

357 Li, L., Dong, J., Njeudeng Tenku, S., Xiao, X., 2015. Mapping Oil Palm Plantations in Cameroon
358 Using PALSAR 50-m Orthorectified Mosaic Images. *Remote Sensing* 7, 1206.

359 May-Tobin, C., Boucher, D., Decker, E., Hurowitz, G., Martin, J., Mulik, K., Roquemore, S., Stark,
360 A., 2012. Recipes for Success. Solutions for Deforestation-Free Vegetable Oils, Union of
361 Concerned Scientists (UCS), MA, U.S.A.

362 Miettinen, J., Liew, S.C., 2010. Separability of insular Southeast Asian woody plantation species in
363 the 50 m resolution ALOS PALSAR mosaic product. *Remote Sensing Letters* 2, 299-307.

364 Morel, A.C., Saatchi, S.S., Malhi, Y., Berry, N.J., Banin, L., Burslem, D., Nilus, R., Ong, R.C., 2011.
365 Estimating aboveground biomass in forest and oil palm plantation in Sabah, Malaysian Borneo
366 using ALOS PALSAR data. *Forest Ecology and Management* 262, 1786-1798.

367 Mousseau, F., 2013. Herakles Exposed: The Truth behind Herakles Farms. False Promises in
368 Cameroon, Greenpeace International and The Oakland Institute, Oakland, U.S.A.

369 Nkongho, R.N., Feintrenie, L., Levang, P., 2014. Strengths and weaknesses of the smallholder oil
370 palm sector in Cameroon. *Oilseeds & fats Crops and Lipids* 21, D208.

371 Pontius, R.G., Millones, M., 2011. Death to Kappa: birth of quantity disagreement and allocation
372 disagreement for accuracy assessment. *International Journal of Remote Sensing* 32, 4407-4429.

373 Santos, C., Messina, J.P., 2008. Multi-sensor data fusion for modeling African palm in the Ecuadorian
374 Amazon. *Photogrammetric Engineering and Remote Sensing* 74, 711-723.

375 Santoso, H., Gunawan, T., Jatmiko, R.H., Darmosarkoro, W., Minasny, B., 2011. Mapping and
376 identifying basal stem rot disease in oil palms in North Sumatra with QuickBird imagery.
377 *Precision Agriculture* 12, 233-248.

378 Shafri, H.Z.M., Hamdan, N., Saripan, M.I., 2011. Semi-automatic detection and counting of oil palm
379 trees from high spatial resolution airborne imagery. *International Journal of Remote Sensing* 32,
380 2095-2115.

381 Sheil, D., Casson, A., Meijaard, E., Noordwijk, M.v., Gaskell, J., Sunderland-Groves, J., Wertz, K.,
382 Kanninen, M., 2009. The impacts and opportunities of oil palm in Southeast Asia: What do we
383 know and what do we need to know?, CIFOR, Bogor, Indonesia,

384 Srestasathiern, P., Rakwatin, P., 2014. Oil Palm Tree Detection with High Resolution Multi-Spectral
385 Satellite Imagery. *Remote Sensing* 6, 9749.

386 Tata, H.L., van Noordwick, M., Mulyoutami, E., Rahayu, S., Widayati, A., Mulia, R., 2010. Human
387 livelihoods, ecosystem services and the habitat of the Sumatran orangutan: rapid assessment in
388 Batang Toru and Tripa., World Agroforestry Centre (ICRAF) Southeast Asia Regional
389 Office, Bogor, Indonesia.

390 Thenkabail, P.S., Stucky, N., Griscom, B.W., Ashton, M.S., Diels, J., van der Meer, B., Enclona, E.,
391 2004. Biomass estimations and carbon stock calculations in the oil palm plantations of African
392 derived savannas using IKONOS data. *International Journal of Remote Sensing* 25, 5447-5472.

393 Uryu, Y., Mott, C., Foead, N., Yulianto, K., Budiman, A., Setiabudi, B., Takakai, F., Naursamsu,
394 Sunarto, Purastuti, E., Fadhli, N., Hutajulu, C.M.B., Jaenicke, J., Hatano, R., Siegert, F., Stüwe,
395 M., 2008. Deforestation, degradation, biodiversity loss and CO2 emission in Riau, Sumatra,
396 Indonesia, World Wildlife Fund (WWF), Washington D.C.

397 Wich, S., Yayasan, R., Jenson, J., Refisch, J., Nellemann, C., 2011. Orangutans and the Economics of
398 Sustainable Forest Management in Sumatra, UNEP/GRASP/PanEco/YEL/ICRAF/GRID-Arendal,

399 Wich, Serge A., Garcia-Ulloa, J., Kühl, Hjalmar S., Humle, T., Lee, Janice S.H., Koh, Lian P., 2014.
400 Will Oil Palm's Homecoming Spell Doom for Africa's Great Apes? *Current Biology* 24, 1659-
401 1663.

402 World Bank, 2010. Improving the Livelihoods of Palm Oil Smallholders: the Role of the Private
403 Sector, International Finance Corporation, World Bank Group, Washington DC, USA.

404 World Bank, 2011. The World Bank Group Framework and IFC Strategy for Engagement in the Palm
405 Oil Sector, International Finance Corporation, Washington DC, USA.
406

407 **Tables**

408 **Table 1.** GEE's classifier algorithms which were used in our study.

| Classifier | Description |
|--|---|
| Classification and Regression Trees (CART) | CART is a non-parametric decision tree learning technique which produces prediction models from training data. The models are obtained by recursively partitioning the data space and fitting a simple regression or classification model within each partition to predict continuous or categorical dependent variables respectively. |
| Random Forests (RFT) | Random forests are an ensemble learning method which generates successive decision trees that are independently constructed using a random sample of the data. The best split at each node of the decision tree is based on a subset of randomly selected predictor variables. The number of trees required for a robust result depends on the number of predictors. The GEE default input parameters used for the Random Forest classifier were: number of Rifle decision trees to create per class = 1; number of variables per split = square root of the number of variables; minimum size of a terminal node = 1; and fraction of input to bag per tree = 0.5. |
| Minimum Distance (MD) | Minimum Distance uses spectral characteristics of the training samples which have been chosen as representatives of the different object classes. The Euclidean Distance between the candidate pixel values and the mean values of each class is calculated and the candidate pixel is allocated to the class with the shortest Euclidean Distance. |

409

410

411 **Table 2.** Overall accuracy and Kappa coefficient for GEE classified maps produced by
 412 classifiers CART, RFT and MD using different combinations of spectral bands (RGB, NIR,
 413 SWIR, TIR, ALL). Table ranked based on descending overall accuracy.
 414

| Bands | Classifier | Overall accuracy | Kappa coefficient |
|--------------|-------------------|-------------------------|--------------------------|
| ALL | CART | 93.6% | 0.92 |
| ALL | RFT | 91.2% | 0.89 |
| RGB | CART | 84.9% | 0.82 |
| RGB | RFT | 81.2% | 0.77 |
| SWIR | CART | 70.1% | 0.64 |
| SWIR | RFT | 66.5% | 0.60 |
| SWIR | MD | 63.6% | 0.56 |
| RGB | MD | 62.6% | 0.55 |
| TIR | CART | 62.3% | 0.55 |
| ALL | MD | 59.7% | 0.52 |
| TIR | RFT | 57.0% | 0.48 |
| TIR | MD | 56.3% | 0.47 |
| NIR | MD | 46.9% | 0.36 |
| NIR | CART | 45.5% | 0.35 |
| NIR | RFT | 39.0% | 0.27 |

415

416 **Table 3.** Producer's (%) and User's (%) accuracy of GEE classified maps for all land cover classes using different spectral bands and classifiers.
 417 'Prod' refers to Producer's accuracy and 'User' refers to User's accuracy. Shaded and underlined values represent the three highest values for
 418 immature and mature oil palm producer's and user's accuracy.
 419

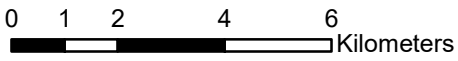
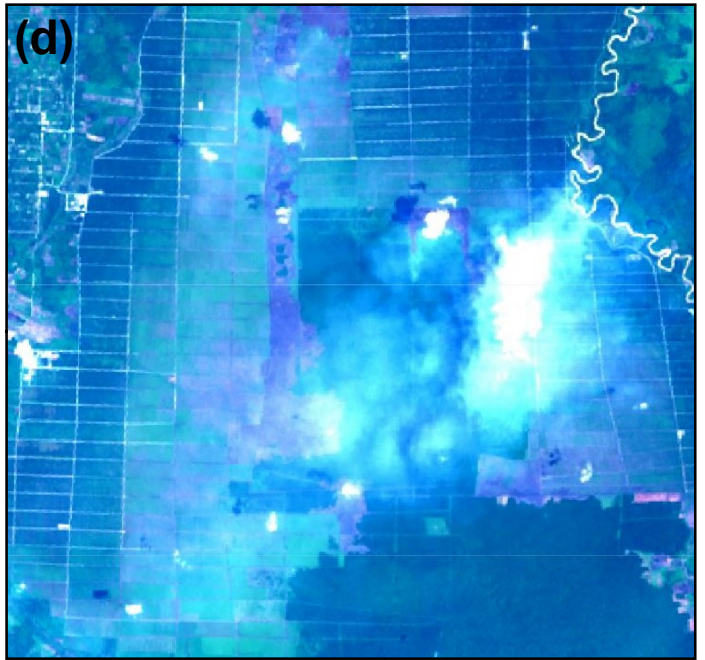
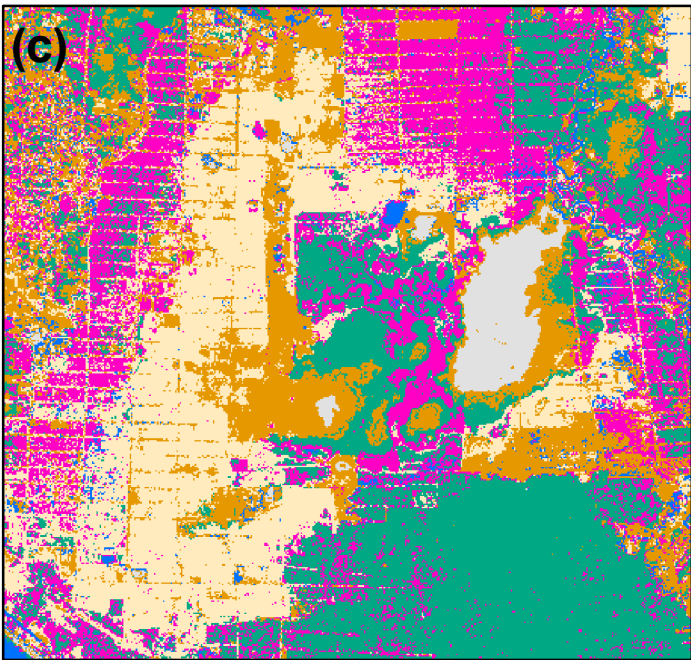
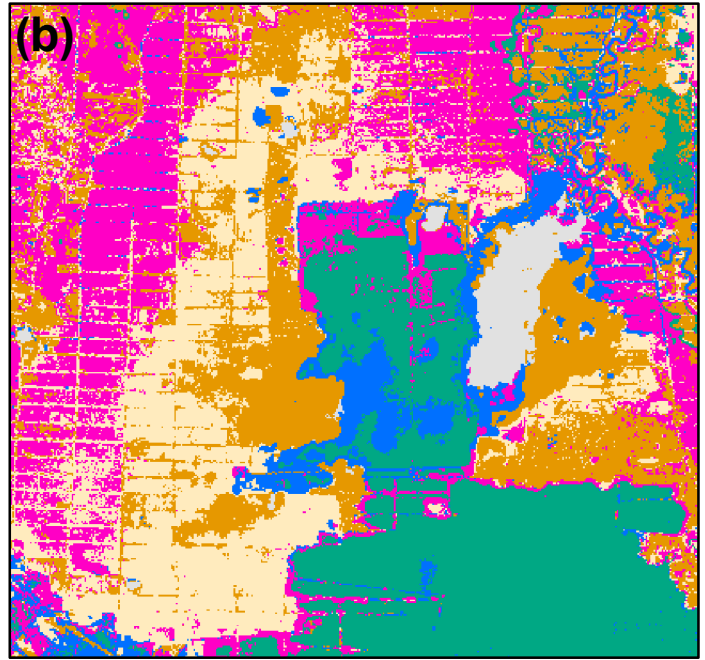
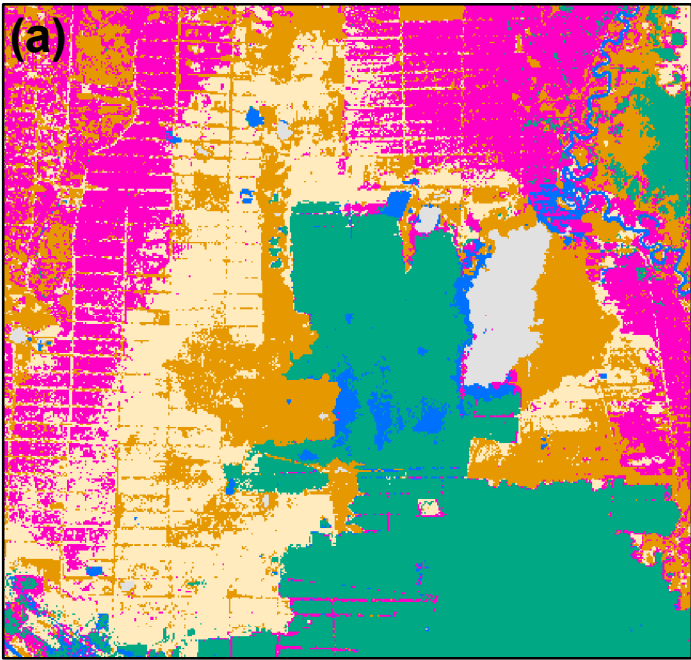
| Bands | Classifier | Land classes | | | | | | | | | | | |
|-------|------------|-------------------|------------|-----------------|------------|-------------------------|------|--------|------|-------|------|--------|------|
| | | Immature Oil Palm | | Mature Oil Palm | | Non-forest non-oil palm | | Forest | | Water | | Clouds | |
| | | Prod | User | Prod | User | Prod | User | Prod | User | Prod | User | Prod | User |
| ALL | CART | <u>94%</u> | <u>88%</u> | <u>88%</u> | <u>88%</u> | 87% | 92% | 99% | 98% | 96% | 97% | 97% | 98% |
| | RFT | <u>88%</u> | 84% | <u>80%</u> | <u>87%</u> | 85% | 81% | 98% | 99% | 96% | 97% | 100% | 98% |
| | MD | 22% | 32% | 72% | 60% | 53% | 43% | 78% | 63% | 72% | 69% | 56% | 100% |
| RGB | CART | 82% | <u>92%</u> | 77% | 70% | 80% | 80% | 85% | 78% | 87% | 93% | 99% | 98% |
| | RFT | <u>83%</u> | <u>86%</u> | 72% | <u>71%</u> | 68% | 74% | 85% | 76% | 81% | 83% | 98% | 97% |
| | MD | 80% | 64% | 68% | 57% | 49% | 72% | 63% | 56% | 57% | 49% | 58% | 99% |
| SWIR | CART | 66% | 57% | 65% | 59% | 70% | 66% | 94% | 92% | 84% | 85% | 39% | 58% |
| | RFT | 48% | 52% | 65% | 56% | 58% | 60% | 94% | 92% | 82% | 87% | 50% | 51% |
| | MD | 57% | 51% | <u>82%</u> | 54% | 29% | 55% | 100% | 81% | 77% | 95% | 36% | 45% |
| TIR | CART | 54% | 52% | 62% | 69% | 50% | 55% | 79% | 68% | 62% | 64% | 67% | 66% |
| | RFT | 49% | 49% | 56% | 58% | 46% | 43% | 66% | 69% | 61% | 60% | 66% | 66% |
| | MD | 28% | 42% | 76% | 59% | 50% | 44% | 76% | 56% | 66% | 60% | 43% | 96% |
| NIR | CART | 20% | 28% | 49% | 37% | 35% | 45% | 66% | 55% | 67% | 62% | 35% | 39% |
| | RFT | 20% | 25% | 45% | 36% | 30% | 31% | 48% | 44% | 57% | 64% | 35% | 34% |
| | MD | 20% | 29% | 23% | 41% | 32% | 37% | 77% | 54% | 65% | 63% | 63% | 45% |

420





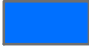

421 **Figure Caption**

422

423 **Figure 1.** Classification results of Classification and Regression Trees (CART) using ALL
424 bands (a), Random Forests (RFT) using ALL bands (b), and CART using RGB bands (c) of
425 Landsat 8 TOA image from 2014 (d).



Legend

-  Immature Oil Palm
-  Mature Oil Palm
-  Non-Oil Palm, Non-Forest
-  Forest
-  Water
-  Clouds